RESEARCH REPORT

FROM THE MICHIGAN STATE UNIVERSITY AGRICULTURAL EXPERIMENT STATION EAST LANSING

Influence of Tapping Techniques on Maple Sap Yields[1]

By PUTNAM W. ROBBINS, Forestry Department

MANY FACTORS are suspected to have pronounced influence on the rates of flow, yields and quality of maple sap. Among these are: 1. the aspect, or compass orientation of the taphole; 2. taphole position in respect to major roots, and height above ground; 3. the diameter and depth of the taphole; 4. the design of the spout; and 5. the relationship of weather to sap flow.

Reliable literature analyzing these factors is lacking, so the following studies were undertaken to determine their roles. To eliminate possible biased conditions of previous tapping, the Baker woodland containing untapped sugar maple trees was selected for the study. This woodland, located on the Michigan State University campus, is typical of sugar bushes of Southern Michigan. In addition, its proximity to the Michigan Section, U. S. Weather Bureau facilitated the incorporation of essential daily meteorological observations with maple sap yield data.

EXPERIMENTAL METHODS

Tree selection

One hundred and twenty-four sugar maples *(Acer saccharum)* having a diameter of 10 inches or more at breast height were selected and numbered. Each of these selected trees was classified according to its diameter at breast height, crown volume and vigor. These classifications and all subsequent data were recorded on I.B.M. cards. From these 124 trees those that were to receive similar treatments were grouped at random with an equal number of tapholes in each class for each treatment. This study was conducted during the sap flow period of three consecutive seasons to minimize differential yield values.

Taphole and tapping

Holes were drilled with a hand brace using 7/16-inch tapping bits, except for the portion of the study covering diameters of different sizes. The holes were drilled at least 24 hours in advance of the first sap flow, based on the maple sap weather forecasts given by the Weather Bureau and the author.

The sap flowed from the taphole to metal buckets or plastic bags through a variety of commercially accepted sap spouts described below. Each day of flow the sap was weighed to the nearest tenth of a pound. Degrees Brix of the maple sap from each tree was measured using a hand refractometer. Finally, the sap was boiled to standard density sirup in a steam jacketed kettle, and judged for flavor and color.

Data processing

The data obtained for each of the three seasons was analyzed using standard analysis of variance with a two-way classification. The data for the three years were combined to provide a final analysis of a three classification scheme with each year corresponding to a replication.

[1] A report of work under contract No. A-1s-33459, United States Department of Agriculture and authorized by the Research and Marketing Act of 1946. The contract is supervised by the Eastern Utilization Research and Development Division of the Agricultural Research Service.

Table 2. Analysis of variance sap yield vs. depth of taphole

Source	Degrees Freedom	Mean Square	"F" Value
Total	143	—	—
Year	2	196,962	26.6*
Depth	2	70,256	9.6
D x Y	4	2,308	0.3
Position	3	5,582	0.8
P x Y	6	5,309	0.7
D x P	6	2,609	0.4
D x Y x P	12	7,861	1.1
Error	108	7,392	—

*Significant at the 5 percent level.

Ecological conditions vs. maple sap flow

Maple sap production was compared to the maximum and minimum temperatures during each 24 hour period and the results are illustrated in Fig. 2. It is for the first season, but typical of the remaining two seasons. The production peaks, as shown in Fig. 2, occurred when cold periods well below 30° F. were followed by daytime temperatures well above 40° F. The graph also shows that a heavy run of sap may be secured early in the season, and that a large, early sap run does not exclude the possibility of large runs later in the season.

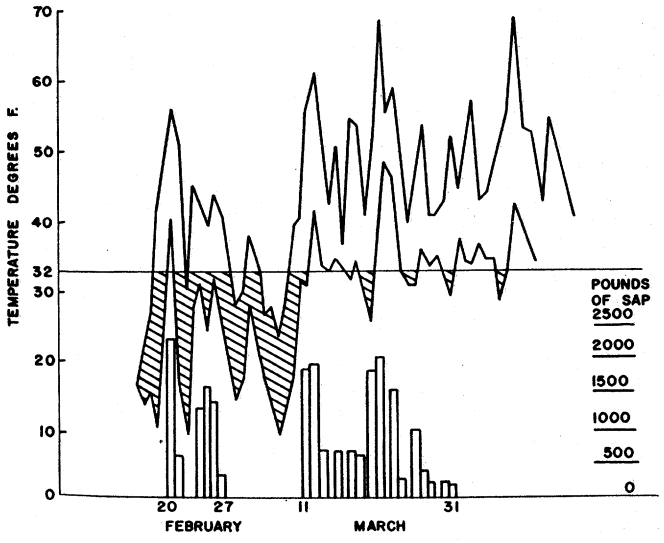

Fig. 2. Temperature Effect On Maple Sap Flow and Yield

In this case the second and third largest flows of sap occurred 20 and 29 days respectively after the heavy run on February 20th. The second season sap started flowing on February 15. Thirty-three days later the largest flow of the season was recorded. The next season good flows were secured in February and early March, however, the largest flow of the season came 41 days after the trees were first tapped. This does not prescribe the sap flow period, but does confirm common knowledge that good maple sap flows are assured when freezing nights are followed by daytime temperatures of 40° F. or higher.

Other ecological factors such as wind velocity, barometric pressures, the growing season, total precipitation and total snowfall were studied over the three seasons. However, no apparent correlation between these ecological factors and the yield of maple sap were demonstrated.

SUMMARY

(1) Maple trees used for the production of sap should be tapped in all four aspects, as there is no difference in quality or significant difference in yields according to the compass position of the taphole to justify concentration of holes in any particular aspect.

(2) Tapholes located over a major root do not produce greater volumes of maple sap.

(3) Tapholes at a height of two and three feet produce more sap than holes located at one foot height. There is no significant difference between yields from tapholes at two foot as compared to three foot levels.

(4) The four commercially designed spouts produce no significant differences in sap yields or sugar yields over one another.

(5) The largest sap yields were obtained from tapholes four inches deep when compared to two and six-inch depth holes.

(6) Taphole diameters larger than 7/16-inch produce no significant increase in maple sap yields.

Compass aspect of taphole

The effect of aspect (compass direction) on the location of the taphole and the volume and quality of sap produced was determined by recording the yields of sap from 168 holes, with 42 holes each on the north, east, south and west. The same trees were tapped for three successive seasons. But the new holes were bored four inches to the left of the preceding year's hole to eliminate any effect resulting from dead wood surrounding the old hole.

No significant difference between quadrants as related to maple sap yield or quality was observed (Fig. 1, Table 1). Robbins[2] reported that any significance in sap yields by compass position would be unlikely.

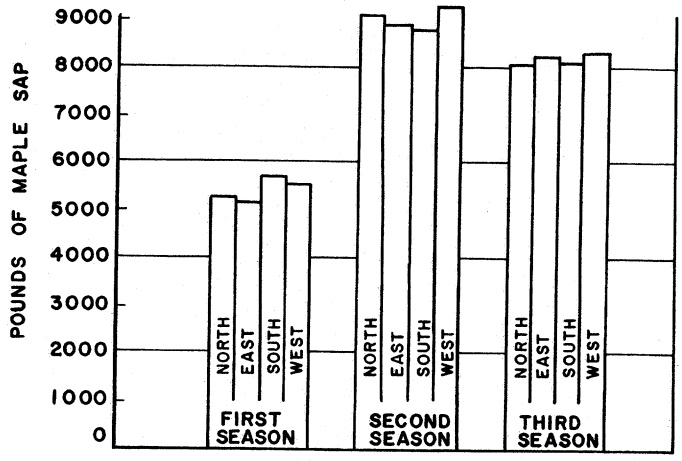

Fig. 1. Aspect and maple sap yields in pounds by position

Table 1. Effect of aspect of taphole on yield and quality

	Aspect Or Compass Position							
	North		East		South		West	
Season	Lbs. of Sap	Quality	Lbs. of Sap	Quality	Lbs. of Sap	Quality	Lbs. of Sap	Quality
1	5245	Good	5168	Good	5844	Good	5566	Good
2	8169	Good	8336	Good	8191	Good	8312	Good
3	9104	Good	9053	Good	8938	Good	9388	Good

Basis: 42 tapholes each season in each of the four positions.
Conclusion: No significant differences in the yield of maple sap by aspect were demonstrated.

Taphole location

To determine the optimum location of the taphole in relation to major roots and the height of the hole above ground, 12 trees in the 20-inch diameter class were tapped. Each tree had three tapholes located over a major root at heights of one, two and three feet. The holes were offset from one another to minimize flow interference. Sap yields were compared to controls from 16 additional trees tapped at two and three feet, but not over a major root.

Sap yields showed a significant relationship to height of tapping during the first two seasons, but not during the third. The two and three foot height holes produced the greatest quantity of sap, while the one foot height produced the smallest volume of sap. This may be attributed to the one foot height holes being occasionally covered by snow and ice, while the two and three foot height holes were free of ice and flowing.

Analysis of the data showed there was no justification of locating tapholes above a major root, when comparing yields or quality of maple sap.

Spout design

Sirup producers and equipment suppliers often claim that a particular type spout is superior to others. To determine the difference in yield of sap, if any, due to the design of spout, four commonly used sap spouts were tested over a period of three seasons. The types[3] were: "Grimm," "LHoir," "Soule" and "Warner." Each was inserted in a minimum of three tapholes in each of four aspects: north, east, south and west making a total of 48 holes in the test.

The yield data, when analyzed for the individual seasons and for the three seasons combined, showed no significant difference due to any particular design of sap spout.

Taphole depth

To determine if tapping deeper than the normal 1 to 1½-inches will produce greater volumes of sap, 16 trees were tapped with 2-inch, 16 with 4-inch and 16 with 6-inch holes. Analysis of the sap yields vs. depth of the taphole showed that the 4-inch depth was significantly greater than the 2-inch and 6-inch depth (Table 2). Morrow[4] reported that tapping depth influenced sap flow less than the number of tapholes per tree.

Taphole diameter

To determine the effect of the size of the taphole on the volume and quality of sap produced, trees were tapped with 7/16, 11/16 and 15/16-inch holes, with 12 trees assigned for each diameter. No significant differences were demonstrated in the sap yields or quality from the different diameters tested.

[2] Robbins, P. W., B. Cool and Jerry Williams. (1955). Final Report on maple sap and syrup. Cooperative Research Project No. A-1s-33459, with Agricultural Research Service, U. S. Dept. of Agriculture. Philadelphia. 46 pp.

[3] Inclusion of commercial trade names does not imply endorsement, approval or recommendation by Michigan State University.

[4] Morrow, Robert R. (1963). Influence of number and depth of tap holes on maple sap flow. Cornell Univ. Agric. Expt. Sta. Bul. 982. 12 pp.

Table 7. *Non-bonded intramolecular distances less than* 3 Å

C(1) H(2)	2·04 Å	C(5) O(2)	2·98 Å
C(1) C(5)	2·40	C(6) H(1)	1·99
C(1) C(3)	2·41	C(6) O(2)	2·32
C(1) C(7)	2·47	C(6) O(1)	2·41
C(1) C(4)	2·81	C(6) N	2·49
C(2) H(1)	2·12	C(6) O(4)	2·79
C(2) H(3)	2·15	C(7) O(3)	2·29
C(2) C(4)	2·42	C(7) H(1)	2·51
C(2) C(6)	2·42	C(7) O(4)	2·71
C(2) C(5)	2·76	C(7) N	2·99
C(3) H(2)	2·14	O(1) O(2)	2·26
C(3) H(4)	2·17	O(1) O(3)	2·54
C(3) C(5)	2·40	O(1) H(1)	2·78
C(3) C(6)	2·80	O(2) H(5)	2·16
C(4) H(3)	2·03	O(2) O(4)	2·85
C(4) C(6)	2·45	O(4) O(5)	2·17
C(4) N	2·45	O(5) H(4)	2·42
C(4) O(5)	2·74	N H(4)	2·60
C(5) H(4)	2·12	H(1) H(2)	2·40
C(5) O(4)	2·32	H(2) H(3)	2·57
C(5) O(5)	2·32	H(3) H(4)	2·38
C(5) C(7)	2·55		

Table 8. *Some planes of atoms*

Atoms	Coefficients* in $AX+BY+CZ+D=0$			
	A	*B*	*C*	*D*
C(1), C(2), C(3), C(4), C(6)	−0·0447	0·0387	0·9983	5·473
O–C=O	0·5341	0·6611	0·5269	2·666
C–O–O	0·6072	0·6079	0·5117	2·552
O–O–H	0·2658	0·3494	0·8985	4·059
O–O · · · O′=	0·3476	0·4156	0·8405	3·850
Nitro group	0·3099	−0·2670	0·9125	5·934

* Referred to the orthogonal axes *abc**.

89° and 146°. In this respect it is noteworthy that in the hydrogen bonded peroxide structures, peroxypelargonic acid and $CONH_2.H_2O_2$, the angle is ~133° and ~106°, respectively, based upon the acceptor oxygen position (Belitskus & Jeffrey, 1965; Lu, Hughes & Giguère, 1941).* These data strongly suggest that the intermolecular hydrogen bond determines the value of the dihedral angle, for the most part, in these peroxides in the solid state. Certainly the exchange repulsions between the lone pair electrons on the peroxide oxygen atoms have a much weaker effect upon the assumed molecular conformation. The estimates of the rotational barrier appearing in the literature have been summarized (Amako & Giguère, 1962). The empirical values listed for the *trans* barrier are 0·32 kcal.m^{-1} from microwave spectra and 0·86 kcal.m^{-1} from infrared rotation spectra. Indeed these results are consistent with the aforementioned point of view.

The torsional angle about the C–O bond, which is the dihedral angle between the OCO and COO planes, has been the subject of speculation in connection with the interpretation of the electric moment data obtained from the monomeric aliphatic peroxyacids in dilute non-polar solvents (Verderame & Miller, 1962). In crystalline *o*-nitroperoxybenzoic acid its value is 5°. The sense of the angle is such that the H atom and the carboxyl oxygen atom are on opposite sides of the COO plane. The oxygen atom is displaced 0·09 Å out of the plane. The bond lengths and valence angles in the peroxycarboxyl group indicate that resonance in the OCO group is not as pronounced as in the carboxylic acid dimers.

A χ^2 test (Hoel, 1947) showed the distances of the ring atoms from a calculated least-squares plane to be significant at the >99% level. Five of the ring atoms are coplanar but the carbon atom bearing the nitro substituent is 0·025 Å (5σ) from this plane. The

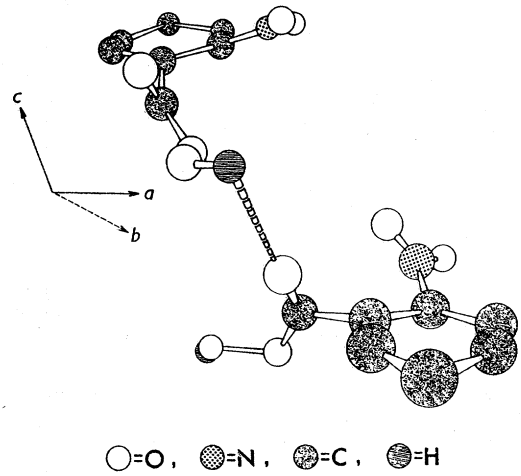

Fig. 3. Perspective view of glide related molecules in a hydrogen bonded chain.

* Also the *trans* configuration for the H_2O_2 molecule has been reported by Pedersen & Pedersen, 1963, in a preliminary discussion of the crystal structure of $Na_2C_2O_4.H_2O_2$. They point out that the *trans* configuration could well be stabilized by two hydrogen bonds to the oxalate ions.

Table 9. *Molecular dihedral angle in H-bonded peroxides and the dihedral angle based upon the H-bond acceptor atom*

Compound	Molecular dihedral angle		Dihedral angle based on acceptor O		
	Atomic planes	Angle	Atomic planes	Angle	
H_2O_2	H–O–O and O–O–H	89°	O · · · O–O and O–O · · · O	93·8°	Busing & Levy, 1958; Abrahams, Collin & Lipscomb, 1951
$H_2O_2.2H_2O$	H–O–O and O–O–H	130	O · · · O–O and O–O · · · O	139	Olovsson & Templeton, 1960
o-Nitroperbenzoic acid	C–O–O and O–O–H	146	C–O–O and O–O · · · O	153	

nitrogen atom is displaced 0·154 Å (30σ) in the same direction. The bond joining the benzene ring to the peroxycarboxyl carbon atom is directed toward the opposite side of plane but toward the same side as the peroxide group (Figs. 2 and 3), and 0·074 Å (15σ) is the distance of the peroxycarboxyl carbon atom from the plane. Evidently steric repulsion exists between the substituent groups. The plane of the ring atoms makes a 58° angle with the OCO plane and a 28° angle with the ONO plane. The valence angles within the benzene ring average 120° (e.s.d. 0·5°) but the angles involving the carbon atom bearing the nitro group deviate significantly (4σ) from this value. Two of the bonds on opposite sides of the ring average 1·385 Å and the other four bonds average 1·399 Å. The significance (2σ) of this difference is questionable. The largest of the three angles subtended at C(5) is C(6)C(5)N and at C(6) it is C(5)C(6)C(7) (Table 6), again an indication of steric strain involving the substituents. The NO distances in the nitro group average 1·226 Å.

Table 10. *Hydrogen bonding distances and angles*

Distance	(Å)	Angle	(°)
H(5)(I) · · · O(1)(II)	1·63	O(3)(I)–H(5)(I) · · · O(1)(II)	166
O(3)(I) · · · O(1)(II)	2·73	H(5)(I)–O(3)(I) · · · O(1)(II)	8
		O(2)(I)–O(3)(I) · · · O(1)(II)	107

Table 11. *Shortest distances between atoms in neighboring molecules*

H(1)–O(3′)	2·54 Å	$(2_1, 0\bar{1}\bar{1})$*
H(2)–H(5)	2·58	$(1, 0\bar{1}0)$
H(3)–O(5)	2·77	$(2_1, 1\bar{1}1)$
H(4)–O(5)	2·49	$(2_1, 1\bar{1}1)$
H(5)–O(1)	1·63	$(c, 00\bar{1})$
O(1)–O(3)	2·73	$(c, 000)$
O(2)–H(2)	2·84	$(c, 0\bar{1}\bar{1})$
O(4)–H(2)	2·66	$(1, 0\bar{1}0)$
N–H(2)	3·46	$(c, 0\bar{1}\bar{1})$
N–H(3)	3·47	$(c, 0\bar{1}0)$
C(1)–H(5)	3·34	$(\bar{1}, 001)$
C(2)–H(5)	3·13	$(1, 0\bar{1}0)$
C(3)–O(5)	3·40	$(c, 0\bar{1}0)$
C(4)–O(5)	3·20	$(2_1, 1\bar{1}1)$
C(5)–C(2)	3·47	$(c, 0\bar{1}\bar{1})$
C(6)–C(1)	3·57	$(c, 0\bar{1}\bar{1})$
C(7)–H(5)	2·73	$(c, 000)$

* The tabulated distance is from the atom in the first column with coordinates as in Table 3 to the atom in the second column with coordinates from Table 3 transformed according to the parenthesized symmetry operation. The first symbol refers to a $P2_1/c$ group operator for the second setting, and the three integers refer to the lattice translational operation to be applied in the transformation.

Glide related molecules are hydrogen bonded in an infinite chain nearly parallel to the *c* axis (Fig. 3). The distances and angles between atoms involved in the hydrogen bonding system are given in Table 10. The closest intermolecular contacts at each atom are listed in Table 11.

We wish to acknowledge the assistance of Prof. G. A. Jeffrey with this research. We are also grateful to Dr L. Silbert for his interest in the problem.

This research was supported by the U.S. Department of Agriculture under Contract No. 12–14–100–5777(73).

References

Abrahams, S. C., Collin, R. L. & Lipscomb, W. N. (1951). *Acta Cryst.* **4**, 15.

Amako, Y. & Giguère, P. A. (1962). *Canad. J. Chem.* **40**, 765.

Belitskus, D. & Jeffrey, G. A. (1965). *Acta Cryst.* In the press.

Berghuis, J., Haanappel, IJ. M., Potters, M., Loopstra, B. O., MacGillavry, C. H. & Veenendaal, A.L. (1955). *Acta Cryst.* **8**, 478.

Beurskens, P. T. (1963). Techn. Report on Sign Correlation by the Sayre Equation. The Crystallography Lab., University of Pittsburgh, Pittsburgh, Pa.

Beurskens, P. T. (1965). In the press.

Busing, W. R. & Levy H. A. (1958). *Amer. Cryst. Assoc.* Meeting Abstr.

Hauptman, H. & Karle, J. (1953). *Solution of the Phase Problem. I. The Centrosymmetric Crystal.* A. C. A. Monograph No. 3. Brooklyn: Polycrystal Book Service.

Hoel, P. G. (1947). *Introduction to Mathematical Statistics.* New York: Wiley.

Karle, I. L. Hauptman, H., Karle, J. & Wing, A. B. (1958). *Acta Cryst.* **11** 257.

Lobunez, W., Rittenhouse, J. R. & Miller, J. G. (1958). *J. Amer. Chem. Soc.* **80**, 3505.

Lu, C. S., Hughes, E. W. & Giguère, P. A. (1941). *J. Amer. Chem. Soc.* **63**, 1507.

McWeeny, R. (1951). *Acta Cryst.* **4**, 513.

Olovsson, I. & Templeton, D. H. (1960). *Acta Chem. Scand.* **14**, 1325.

Pedersen B. F. & Pedersen, B. (1963). *Acta Cryst.* **16**, A 75.

Rittenhouse, J. R., Lobunez, W., Swern, D. & Miller, J. G. (1958). *J. Amer. Chem. Soc.* **80**, 4850.

Swern, D. & Silbert, L. S. (1963). *Anal. Chem.* **35**, 880.

Swern, D., Witnauer, L. P., Eddy, C. R. & Parker, W. E. (1955). *J. Amer. Chem. Soc.* **77**, 5537.

Verderame, F. D. & Miller, J. G. (1962). *J. Phys. Chem.* **66**, 2185.

clearly revealed the atomic positions was calculated with the use of these 441 reflexions (Fig. 2). Structure factors calculated with these coordinates and the single overall temperature factor, $B=2{\cdot}52$ Å^2, gave an R value of 25·3% on 1277 reflexions.

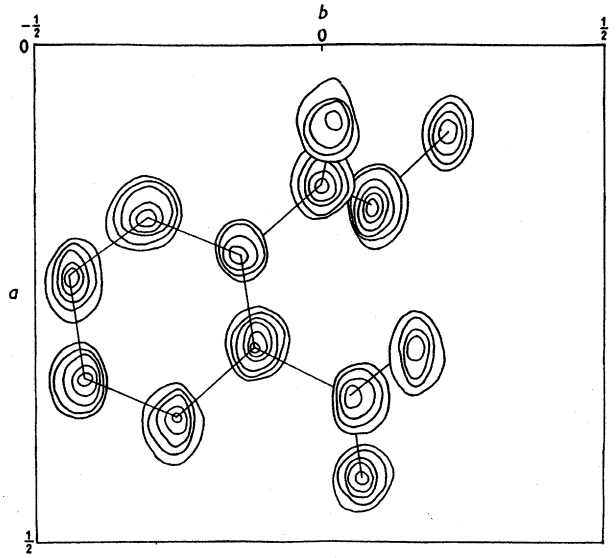

Fig. 2. Composite E map. Scale arbitrary.

Structure refinement

The coordinates obtained from the E map were refined in three cycles of differential synthesis holding the temperature and scale factor constant, the IBM 7070 program of Shiono being used. A cycle of anisotropic differential synthesis lowered the agreement index to 18·1. A difference Fourier synthesis yielded the positions of three of the four hydrogen atoms attached to the aromatic ring, but the acidic hydrogen could not be located unequivocally. Knowledge of the site of this hydrogen was important, for it completes the structural information required to determine the conformation of the peroxycarboxyl group and to estimate the influence of the intermolecular hydrogen bond upon it. Six more cycles of anisotropic differential syntheses lowered the agreement index to 12·9, but the site of the acidic hydrogen was still undetermined although all of the hydrogen atoms attached to the ring could now be located in the difference map.

Up to this point all of the data had been used in the refinement. All reflexions that could not be observed above the background plus forty-one reflexions with observed intensity less than two on the arbitrary scale were dropped from subsequent refinement cycles. The intensity data for the forty-one reflexions were obtained from only one setting of the crystal (about one axis), and the $|F_o-F_c|$ values showed that they were not accurately estimated. Two cycles of anisotropic differential synthesis lowered the agreement index to 12·0 on 1237 reflexions.

Table 4. *Anisotropic temperature coefficients**

Atom	Differential synthesis					Least squares						σ (Å^2)					
	B_{11}	B_{22}	B_{33}	B_{12}	B_{13}	B_{23}	B_{11}	B_{22}	B_{33}	B_{12}	B_{13}	B_{23}	B_{11}	B_{22}	B_{33}	B_{12}	B_{13}	B_{23}
C(1)	2·03	0·94	1·68	−0·32	0·70	0·23	2·54	1·33	2·06	−0·50	0·89	0·29	0·18	0·18	0·16	0·15	0·14	0·14
C(2)	3·21	0·70	2·40	−0·26	0·95	−0·11	3·62	0·85	2·31	−0·32	1·04	0·08	0·19	0·16	0·17	0·15	0·14	0·15
C(3)	3·02	1·64	2·36	0·48	0·98	−0·40	3·37	1·53	2·82	0·09	1·25	−0·52	0·19	0·16	0·15	0·15	0·13	0·13
C(4)	2·35	1·62	2·34	0·29	1·13	0·04	2·42	1·71	2·60	0·05	1·08	−0·06	0·17	0·20	0·16	0·15	0·13	0·15
C(5)	2·29	1·12	1·85	0·09	0·71	−0·18	2·31	1·35	1·91	−0·13	0·63	−0·13	0·21	0·20	0·19	0·18	0·17	0·16
C(6)	2·26	0·78	1·62	0·13	0·75	−0·25	2·28	0·90	1·67	0·22	0·63	−0·11	0·18	0·21	0·18	0·14	0·15	0·15
C(7)	2·02	0·80	2·22	0·29	0·75	−0·08	2·59	0·97	2·31	0·46	0·75	−0·07	0·22	0·17	0·18	0·16	0·17	0·14
O(1)	3·99	2·56	3·03	1·27	2·12	0·38	4·34	2·76	3·27	1·44	2·36	0·52	0·20	0·18	0·16	0·15	0·15	0·14
O(2)	3·16	1·87	3·54	1·36	2·10	1·53	3·54	2·06	3·79	1·47	2·08	1·57	0·22	0·16	0·29	0·15	0·22	0·18
O(3)	3·70	2·39	7·20	1·91	3·40	3·14	3·68	2·63	7·14	2·05	3·05	3·04	0·17	0·16	0·18	0·14	0·14	0·14
O(4)	4·25	1·69	6·21	−0·43	2·12	−0·87	4·73	1·50	6·65	−0·25	2·42	−0·93	0·21	0·21	0·22	0·17	0·17	0·17
O(5)	3·95	3·02	4·53	−1·51	2·13	0·05	4·27	3·33	4·90	−1·84	2·39	−0·16	0·19	0·18	0·29	0·16	0·19	0·20
N(1)	2·10	1·16	2·87	−0·66	0·39	0·32	2·86	1·60	3·23	−0·63	0·58	0·53	0·18	0·18	0·18	0·14	0·21	0·15

* In the form $f^0(hkl)\exp[-\frac{1}{4}(B_{11}\cdot h^2a^{*2}+\ldots+B_{23}\cdot 2klb^*c^*)]$.

Two cycles of full-matrix least-squares refinement were run with the IBM 704 program of Busing & Levy, with the Hughes weighting scheme. Four reflexions showing extinction were omitted from the refinement. The agreement index on 1237 reflexions including the four low order reflexions was virtually unchanged at 11·9, although there were some changes in the parameters, as shown in Tables 3 and 4. The tabulated e.s.d. are those computed in the least-squares method.

Still the site of the acidic hydrogen was obscured in the difference map by errors in the data. A difference Fourier synthesis was then calculated with 417 selected reflexions, for which $|F_o - F_c| < 4{\cdot}0$, $\sin\theta < 0{\cdot}6$, and for which the agreement index was 8·9. A peak of 0·3 e.Å^{-3} containing $\sim 0{\cdot}7$ electron occurred in a stereochemically plausible site for the hydrogen bond. A single spurious maximum of 0·3 e.Å^{-3} containing $\sim 0{\cdot}2$ electron appeared in a position that gave unreasonable distances and angles for the valence bond and hydrogen bond. The estimated standard deviation in the electron density based upon these selected reflexions was 0·095 e.Å^{-2}. The reason that the acidic hydrogen atom was more difficult to find than the four hydrogen atoms linked to the aromatic ring is probably associated with the large thermal parameters of the oxygen atom to which it is bound.

The hydrogen atoms were assigned the same temperature factors as the atoms to which they are bonded. The carbon, oxygen and nitrogen scattering factors were those given by Berghuis, Haanappel, Potters, Loopstra, MacGillavry & Veenendaal (1955). Those of McWeeny (1951) were used for the hydrogen atoms. Unobserved reflexions were omitted from calculations of the R value. The observed and calculated structure factors are given in Table 12.*

Discussion of the structure

The atomic coordinates from the two methods of refinement were averaged and the molecular dimensions were calculated from the mean values. The bond lengths and valence angles are listed in Tables 5 and 6. Some non-bonded intramolecular distances are listed in Table 7. The equations of planes of atoms that are useful in the discussion of the molecular structure are given in Table 8.

The dihedral angle between the COO and the OOH planes is 146°, which is significantly larger than has been reported for other organic peroxides from their electric moments in dilute solution (Verderame & Miller, 1962; Rittenhouse, Lobunez, Swern & Miller, 1958; Lobunez, Rittenhouse & Miller, 1958). A stereochemical feature of the hydrogen bonded peroxides is the relation between the molecular dihedral angle and the dihedral angle calculated with the O–O · · · O plane, that is with the hydrogen bond acceptor atom. These angles are compared in three hydrogen bonded peroxide structures in Table 9. In each case the dihedral angle based upon the acceptor oxygen is greater by a few degrees than the molecular dihedral angle. Nevertheless, in all of these cases the hydrogen atom lies nearly on the line that joins the hydrogen bonded oxygen atoms, even though the molecular dihedral angle is found at values scattered between

Table 5. *Bond lengths in o-nitroperoxybenzoic acid*

Bonded atoms	Distance	σ
C(1)–C(2)	1·399 Å	0·007 Å
C(2)–C(3)	1·379	0·008
C(3)–C(4)	1·401	0·007
C(4)–C(5)	1·397	0·007
C(5)–C(6)	1·390	0·007
C(6)–C(1)	1·401	0·007
C(6)–C(7)	1·495	0·007
C(7)–O(1)	1·214	0·007
C(7)–O(2)	1·337	0·006
O(2)–O(3)	1·478	0·007
C(5)–N(1)	1·478	0·007
N(1)–O(4)	1·236	0·007
N(1)–O(5)	1·215	0·007
C(1)–H(1)	0·96	0·12
C(2)–H(2)	1·02	0·12
C(3)–H(3)	1·03	0·12
C(4)–H(4)	1·06	0·12
O(3)–H(5)	1·12	0·15

Table 6. *Bond angles and their e.s.d. in o-nitroperoxybenzoic acid*

Angle		σ
C(6)C(1)C(2)	119·7°	0·4°
C(1)C(2)C(3)	120·7	0·5
C(2)C(3)C(4)	120·8	0·5
C(3)C(4)C(5)	117·8	0·5
C(4)C(5)C(6)	122·4	0·5
C(5)C(6)C(1)	118·6	0·4
C(1)C(6)C(7)	117·1	0·4
C(5)C(6)C(7)	124·2	0·4
C(6)C(7)O(1)	125·1	0·5
C(6)C(7)O(2)	109·9	0·4
O(1)C(7)O(2)	124·7	0·5
C(7)O(2)O(3)	108·9	0·4
C(5)N(1)O(4)	116·8	0·5
C(5)N(1)O(5)	118·3	0·5
C(6)C(5)N(1)	120·7	0·4
C(4)C(5)N(1)	116·8	0·4
O(4)N(1)O(5)	124·8	0·5
H(1)C(1)C(2)	127	7
C(6)C(1)H(1)	113	7
H(2)C(2)C(3)	125	7
C(1)C(2)H(2)	114	7
H(3)C(3)C(4)	113	7
C(2)C(3)H(3)	126	7
H(4)C(4)C(5)	119	6
C(3)C(4)H(4)	123	6
O(2)O(3)H(5)	112	6

* Table 12 has been deposited as Document number 7999 with the ADI Auxiliary Publications Project, Photoduplication Service, Library of Congress, Washington 25, D.C., U.S.A. A copy may be secured by citing the Document number and remitting \$3·75 for photoprints, or \$2·00 for 35 mm microfilm. Advance payment is required. Make check or money order payable to Chief, Photoduplication Service, Library of Congress.

peroxyesters. Compounds in the first two of these classes are currently being investigated in these laboratories. The crystal structure analysis of *o*-nitroperbenzoic acid (Fig. 1) is reported here as a part of that study. This aromatic peroxy acid was selected because the quality of the crystals indicated that an analysis of this compound would yield more reliable parameters than could be obtained from an aliphatic peroxy acid, although these are also being studied. The main interest in the crystal structure of the peroxy acids stems from the fact that neither the intermolecular hydrogen bonding scheme nor the conformation of the peroxycarboxyl group is known in the solid state (Swern, Witnauer, Eddy & Parker, 1955). In the case of *o*-nitroperbenzoic acid a closely related and pertinent question concerns the influence of the *o*-nitro group upon these two structural features. Finally, the aromatic peroxy acids merit attention, for relatively little work has been published on their structures (Swern & Silbert, 1963).

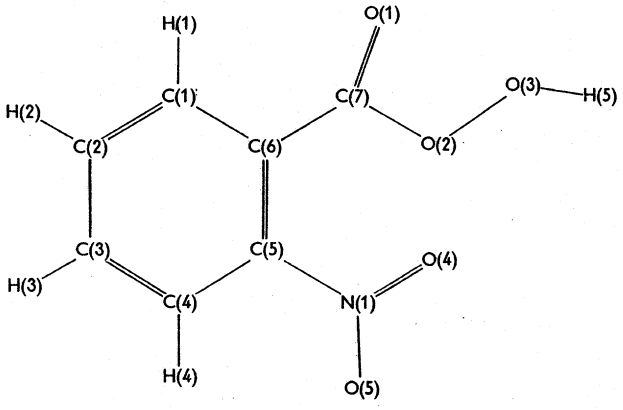

Fig. 1. *o*-Nitroperoxybenzoic acid: the atomic numbering.

Crystal data

o-Nitroperbenzoic acid, $C_7H_5O_5N$; M.W. 183·118, m.p. 95–96 °C.

Monoclinic:

Cell dimensions (25 °C)

$$a=13\cdot84\pm0\cdot02,\ b=8\cdot03\pm0\cdot02,$$
$$c=7\cdot51\pm0\cdot02\ \text{Å};\ \beta=112°\pm30'.$$

Cell dimensions (−15 °C)

$$a=13\cdot75\pm0\cdot02,\ b=7\cdot95\pm0\cdot01,$$
$$c=7\cdot47\pm0\cdot01\ \text{Å};\ \beta=112°\ 40'\pm10'.$$
$$V\ (25\ °C)=773\cdot8\ \text{Å}^3,\ V\ (-15\ °C)=753\cdot5\ \text{Å}^3,$$
$$D_m\ (25\ °C)=1\cdot576\ \text{g.cm}^{-3}.$$
$$Z=4,\ D_x\ (25\ °C)=1\cdot572\ \text{g.cm}^{-3},$$
$$D_x\ (-15\ °C)=1\cdot614\ \text{g.cm}^{-3}.$$

Space group, $P2_1/c$ from systematic extinctions $h0l$ absent l odd; $0k0$ absent k odd.

Experimental

The crystals of *o*-nitroperbenzoic acid were suppl to us by Dr L. Silbert of the Eastern Regional Labo.a- tories, U.S. Department of Agriculture. These had well formed faces and were elongated in the *c* direction. The multifilm equi-inclination Weissenberg photographic method was used, with Cu $K\alpha$ radiation, for collecting the intensity data. Thermal and chemical instability of the compound required a reduced temperature, ~ −15 °C, for the exposures. Data were obtained from single crystals mounted about the three principal axes. Of the 1575 possible independent reflexions within the limiting sphere for Cu $K\alpha$ radiation, 94% were indexed and estimated, and 81% were observed above the background.

The uncorrected intensities were estimated visually by comparison with a standard scale. The data reduction, angle corrections, and interlayer correlations were carried out on the IBM 1620 computer. No extinction or absorption corrections were applied.

The unit-cell parameters were determined from equatorial Weissenberg photographs calibrated with NaCl.

Structure determination

The data were placed on the absolute scale by means of a Wilson plot and the structure amplitudes were corrected for thermal vibration and normalized (Hauptman & Karle, 1953). The sign correlation method (Beurskens, 1963, 1965) was used for solvin the phase problem. In this method several structure factors are, at first, given signs arbitrarily and these together with an appropriate origin-determining set of structure factors are used to generate other signs relative to these initial choices by means of the sign relation

$$sE(h+k)\sim sE(h).sE(k)\ . \qquad (1)$$

At the time this analysis was carried out, however, the number of arbitrary choices allowed by the computer program was restricted to six and the procedure accordingly was initiated more laboriously.

The signs of the reflexions $E(\bar{2}73)$, $E(163)$ and $E(061)$ were selected positive to fix the origin and these were used to obtain signs of the seven reflexions listed in Table 1 with relation (1). On the basis of the following four arguments there was no doubt that

Table 1. *The initial reflexions of the set* [0]

hkl	*E*	Sign
$\bar{2}73$	3·36	[0]+
163	3·13	[0]+
061	2·53	[0]+
002	2·02	[0]−
$\bar{2}75$	2·63	[0]−
$\bar{1}18$	2·50	[0]+
104	2·32	[0]−
$\bar{2}14$	2·20	[0]−
102	2·05	[0]+
$\bar{3}71$	2·03	[0]+

these signs were correct: (1) They were obtained at least once with a high probability ($|E(h)E(k)E(h+k)|$. $N^{-\frac{1}{2}} = Q \geq 2{\cdot}00$, *i.e.* with a probability larger than 98%). (2) Each of these was found at least once again in a relation (1) with a good probability ($Q \geq 1{\cdot}3$). (3) A further expansion to obtain signs for many reflexions ($Q \geq 1{\cdot}0$) did not give rise to any inconsistent relation (1). (4) The sign of the reflexion $E(002)$ was also found by the Σ_1 relation (Hauptman & Karle, 1953) with a probability >98%. These seven reflexions are therefore registered together with the origin-determining reflexions in correlation set [0] (*i.e.* the set of reflexions with known signs).

We then arbitrarily selected the signs of six reflexions with a high E value and registered these in the correlation set [1] through [6] (see Table 2); the given signs were not completely arbitrarily selected since they were based upon the results of a preliminary examination using the procedure to be described immediately. Relation (1) was used with the 16 structure factors in Table 1 and 2 to generate many signs and the dependency of the new signs upon initial choices was traced by the computer program so that they were registered into their appropriate correlation sets. A correlation set $[i, j, \ldots]$ is defined as that set of reflexions with signs that are known to be dependent upon the arbitrary choices numbered $i, j, \ldots$ (Beurskens, 1963). A reflexion which was found several times with a high probability within a particular correlation set was included in the set, and used for further sign generation. Thus 14 signs could be 'accepted' in this way.

From the 385 relations (1) with $Q \geq 1{\cdot}0$ which were now available the correlation equations $[3] \equiv [0]$ and $[2, 6] \equiv [0]$ were found and consequently the third and the sixth arbitrary choices were eliminated. In other words, all reflexions in correlation set [3] were transferred into set [0] and those in set [6] were transferred to set [2]. Thus, the dependency upon choice three is cancelled and that upon choice six is transferred to a dependency upon choice two. It was now possible to proceed in the same way by 'accepting' more signs and eliminating other arbitrary choices, as given in the consecutive columns of Table 2. The last correlation equation $[1] \not\equiv [0]$ indicated that all signs dependent upon choice one should have opposite signs. Thus a single set of 171 signs was obtained and the phase problem was thereby solved.

The list of known phases was extended to 306 structure factors by considering relation (1) with $Q \geq 0{\cdot}8$. Finally, a total of 441 signs were obtained by applying Σ_2 relations with $Q \geq 0{\cdot}6$. An E map (Karle, Hauptman, Karle & Wing, 1958), which

Table 2. *The six arbitrary choices and their sign dependency during the course of the analysis*

Correlation equation			$[3] \equiv [0]$	$[2, 6] \equiv [0]$	$[2, 5] \equiv [0]$	$[1, 2, 4] \equiv [0]$	$[2] \equiv [0]$	$[1] \not\equiv [0]$
No. of choice eliminated			3	6	5	4	2	1
hkl	E	Initial sign						
$\bar{1}\bar{1}$,3,4	3·03	[1]+	[1]+	[1]+	[1]+	[1]+	[1]+	[0]−
171	2·88	[2]+	[2]+	[2]+	[2]+	[2]+	[0]+	[0]+
$\bar{2}$76	2·93	[3]−	[0]−	[0]−	[0]−	[0]−	[0]−	[0]−
$\bar{1}\bar{0}$,2,6	2·85	[4]+	[4]+	[4]+	[4]+	[1, 2]+	[1]+	[0]−
366	2·77	[5]−	[5]−	[5]−	[2]−	[2]−	[0]−	[0]−
072	2·75	[6]+	[6]+	[2]+	[2]+	[2]+	[0]+	[0]+

Table 3. *Atomic coordinates*

Atom	Fractional coordinates Differential synthesis			Least squares			e.s.d. (Å)		
	x	y	z	x	y	z	$\sigma(x)$	$\sigma(y)$	$\sigma(z)$
C(1)	0·1785	−0·3014	0·8098	0·1783	−0·3022	0·8096	0·005	0·005	0·005
C(2)	0·2445	−0·4387	0·8216	0·2451	−0·4381	0·8219	0·006	0·005	0·005
C(3)	0·3456	−0·4133	0·8288	0·3454	−0·4130	0·8291	0·006	0·005	0·006
C(4)	0·3837	−0·2505	0·8254	0·3839	−0·2502	0·8259	0·005	0·005	0·005
C(5)	0·3169	−0·1153	0·8163	0·3175	−0·1152	0·8183	0·005	0·005	0·005
C(6)	0·2148	−0·1376	0·8056	0·2145	−0·1377	0·8056	0·005	0·004	0·005
C(7)	0·1381	0·0025	0·7819	0·1383	0·0023	0·7826	0·005	0·005	0·005
O(1)	0·0900	0·0271	0·8868	0·0912	0·0272	0·8872	0·005	0·004	0·004
O(2)	0·1231	0·0882	0·6196	0·1233	0·0881	0·6198	0·004	0·004	0·004
O(3)	0·0477	0·2263	0·6007	0·0475	0·2257	0·5994	0·005	0·005	0·006
O(4)	0·3264	0·1646	0·9078	0·3253	0·1651	0·9061	0·005	0·004	0·006
O(5)	0·4365	0·0759	0·7848	0·4364	0·0759	0·7845	0·005	0·005	0·005
N(1)	0·3631	0·0552	0·8342	0·3628	0·0550	0·8348	0·005	0·004	0·005
H(1)*				0·105	−0·307	0·790			
H(2)*				0·215	−0·552	0·840			
H(3)*				0·395	−0·505	0·815			
H(4)*				0·460	−0·225	0·830			
H(5)*				0·065	0·340	0·530			

* The hydrogen coordinates were obtained from difference maps.